Acta metall. mater. Vol. 41, No. 4, pp. 1119–1136, 1993
Printed in Great Britain.

0956-7151/93 $6.00 + 0.00

MICROSTRUCTURAL EVOLUTION IN TWO-DIMENSIONAL TWO-PHASE POLYCRYSTALS

E. A. HOLM[1]†, D. J. SROLOVITZ[1] and J. W. CAHN[2]

[1]Department of Materials Science and Engineering, The University of Michigan, Ann Arbor, MI 48109 and [2]Materials Science and Engineering Laboratory, National Institute of Standards and Technology, Gaithersburg, MD 20899, U.S.A.

(Received 19 May 1992; in revised form 16 August 1992)

Abstract—In two-dimensional polycrystals composed of α-phase and β-phase grains the stability of $\alpha\alpha\alpha$, $\beta\beta\beta$, $\alpha\alpha\beta$ and $\alpha\beta\beta$ three-grain junctions and $\alpha\beta\alpha\beta$ four-grain junctions depends on the α–α, β–β and α–β interfacial energies. A computer simulation which generates thermodynamically consistent microstructures for arbitrary interfacial energies has been utilized to investigate microstructural evolution in such polycrystals when phase volume is not conserved. Since grain shapes, phase volume, and phase arrangements are dictated by interfacial energies, clustered-, alternating-, isolated-, and single-phase microstructures occur in different interfacial energy regimes. Despite great differences in microstructure, polycrystals which contain only three-grain junctions evolve with normal grain growth kinetics. In contrast, structures containing flexible four-grain junctions eventually stop evolving. We conclude that two-dimensional polycrystals continually evolve when grain junction angles are thermodynamically fixed, while grain growth ultimately ceases when grain junction angles may vary. Predictions concerning three-dimensional and phase-volume conserved systems are made.

1. INTRODUCTION

A number of important engineering materials, such as composites, precipitate-strengthened materials, and materials with eutectics and/or miscibility gaps in their phase diagrams, are examples of two-phase materials in which each phase may be polycrystalline. In many cases, both phases may evolve under processing or service conditions. Both phase separation and grain growth may occur during microstructural evolution in such materials, and both processes may affect the properties of these materials. For instance, mechanical and electrical properties may rely on the material maintaining a structure in which grains of one or both phases remain either interconnected or distributed throughout evolution; creep properties are affected by the grain size attained by each phase. However, the parameters and processes which control microstructural evolution in two-phase polycrystalline materials have not been systematically examined.

As a first step in investigating such processes, we have studied microstructural evolution in two-dimensional, two-phase polycrystals. Two-dimensional (2-D) systems are chosen for three reasons. First, 2-D systems provide a logical, simple starting place to test the concepts of two-phase grain growth. Second, in two dimensions, grain boundary curvature has a single component κ, and both grain topology (i.e. the number of sides per grain) and grain growth rate depend on that curvature; in three dimensions, curvature has two orthogonal components κ_1 and κ_2, and grain topology depends on the Gaussian curvature of a boundary ($\kappa_1\kappa_2$), while growth rate depends on the geometric curvature ($\kappa_1 + \kappa_2$). Thus, for curvature-driven coarsening processes such as grain growth, some very useful rules relating grain topology and growth rate can be derived in two dimensions which have no known corollaries in three dimensions. Finally, when grain growth is spatially uniform, stereological relationships require that a 2-D system resemble a cross-section of the corresponding three-dimensional (3-D) system (i.e. grain corner angles in 2-D are the same as grain edge angles in 3-D; 3-D point junctions appear with vanishing probability in a 2-D section; etc.). While a 2-D system may not exhibit a number of phenomena unique to 3-D systems, it can nonetheless provide useful insight.

Physically, a 2-D polycrystal may be viewed as a polycrystalline thin film in which the grain size is larger than the film thickness and grain boundary grooving does not occur. In such a system, the grain boundaries may move only in the two in-film-plane dimensions; hence, growth is referred to as 2-D.

We begin our analysis of 2-D grain growth by examining the evolution of a grain surrounded by n neighbor grains. The n sides of the grain are boundary arcs where two grains meet, and the n corners of the grain are point junctions where three or more grains meet. We assume that grain boundaries possess some boundary free energy per unit arc length, γ, which is isotropic with respect to the grain boundary normal direction. In a single phase, energetically isotropic, 2-D system, it may be shown that the only stable grain corner is the three-grain

†Present address: Physical and Joining Metallurgy Department, Sandia National Laboratories, Albuquerque, NM 87185, U.S.A.

junction (trijunction), and the balance of interfacial energies at the trijunction requires that all grain corner angles be $2\pi/3$.

This angular condition at grain corners necessitates that single phase, 2-D grain growth proceed according to a "six minus n" rule, often referred to as von Neumann's rule [1–4]. Because boundary curvature may be defined as the negative rate of change of boundary area with volume swept out by a moving boundary, curvature provides the driving force for the minimization of total grain boundary energy via boundary motion [5]. Hence, von Neumann's rule arises from the assumption that grain boundaries move toward their centers of curvature with velocity V proportional to boundary curvature κ, specifically

$$V = M\kappa \tag{1}$$

where M is the boundary mobility, and the fact that

$$\frac{dA}{dt} = -\int_G V\, ds \tag{2}$$

where A is the area of a 2-D grain, s is grain boundary length, and the integral is over the arcs of grain boundary between grain corners. The integral of the grain boundary curvature around a 2-D grain G is given by

$$\int_G \kappa\, ds + \sum_{i=1}^{n} \theta_i = 2\pi \tag{3}$$

where the grain boundary curvature κ is taken to be positive toward the center of the grain, the integral is taken over the grain boundary arcs, and the θ_i are the complements of the interior angles at each of the n grain corners. If grains meet only at trijunctions with the equilibrium angle of $2\pi/3$, all $\theta_i = \pi/3$, so

$$\frac{dA}{dt} = -M\int_G \kappa\, ds = -M\frac{\pi}{3}(6-n). \tag{4}$$

Equation (4) is von Neumann's rule [1–4]. When von Neumann's rule holds, the rate of change in the area of each grain is governed only by its number of corners and is independent of the grain size and of any properties of the neighboring grains. Hence, a 6-sided grain will neither grow nor shrink, while a 7-sided grain always grows and a 5-sided grain always shrinks.

It is important to emphasize that it is the angular conditions at the grain corners which give rise to the curvature driving force for grain growth. That is, to maintain corner angles of $2\pi/3$ in a 4-sided grain, the integrated curvature of the grain must be positive (i.e. on average, the sides "bow out" from the center of the grain); hence, as the curved boundaries move toward their centers of curvature, the grain shrinks. Conversely, an 8-sided grain has a negative integrated curvature (i.e. sides "bow inward") and therefore must grow. Only a 6-sided grain may have all corner angles equal to $2\pi/3$ with an integrated curvature of zero; thus, only hexagonal grains neither grow nor shrink in a single-phase, isotropic system. While boundary curvature is the driving force for grain growth, it is the angular conditions at grain corners which actually govern the stability of a grain structure.

The presence of two phases (labeled α and β below) necessarily complicates the grain growth problem. Instead of a single grain boundary energy, two boundary free energies ($\gamma_{\alpha\alpha}, \gamma_{\beta\beta}$) and one interfacial free energy ($\gamma_{\alpha\beta}$) control grain junction angles. The dimensionless quantities $R_\alpha = \gamma_{\alpha\alpha}/\gamma_{\alpha\beta}$ and $R_\beta = \gamma_{\beta\beta}/\gamma_{\alpha\beta}$ may be used as parameters which define the relative boundary energetics of the system; alternatively, the interior angle of an α grain at an $\alpha\beta\beta$ trijunction, ϕ_α, and the interior angle of a β grain at an $\alpha\alpha\beta$ trijunction, ϕ_β, provide the same information. These angles may be derived from an interfacial energy force balance, giving [4]

$$\phi_\alpha = 2\cos^{-1}\left(\frac{\gamma_{\beta\beta}}{2\gamma_{\alpha\beta}}\right) = 2\cos^{-1}\left(\frac{R_\beta}{2}\right) \tag{5a}$$

and

$$\phi_\beta = 2\cos^{-1}\left(\frac{\gamma_{\alpha\alpha}}{2\gamma_{\alpha\beta}}\right) = 2\cos^{-1}\left(\frac{R_\alpha}{2}\right). \tag{5b}$$

The thermodynamic stability constraints upon various microstructural features in 2-D, two-phase grain growth were recently analyzed by Cahn [4, 6] and are summarized below.

In a two-phase system, the angles of a same-phase ($\alpha\alpha\alpha$ or $\beta\beta\beta$) trijunction will remain $2\pi/3$ due to the balance of interfacial energies at the trijunction. In an α grain, for example, these single-phase trijunctions are stable for $0 \leqslant R_\alpha \leqslant \sqrt{3}$ (or $\phi_\beta > \pi/3$). When $R_\alpha > \sqrt{3}$, triangular β grains will nucleate spontaneously at all $\alpha\alpha\alpha$ triple points, reducing the total interfacial energy of the system [7–10]. Likewise, the single-phase $\beta\beta\beta$ trijunction is stable for $0 \leqslant R_\beta \leqslant \sqrt{3}$ (or $\phi_\alpha > \pi/3$).

The two-phase trijunction ($\alpha\alpha\beta$ or $\alpha\beta\beta$) is destabilized by wetting. For instance, when $\phi_\alpha = 0$ or $R_\beta \geqslant 2$, phase α penetrates the β–β interface, so the $\alpha\beta\beta$ trijunction (and the β–β interface) is stable only when $0 \leqslant R_\alpha < 2$ (or $\phi_\beta > 0$).

While the stability criteria for trijunctions were discussed by Gibbs [7], the possibility of stable four-grain junctions (quadrijunctions) in two-phase polycrystals was only recently established by Cahn [4, 6]. The angles at which boundaries meet in a quadrijunction are not uniquely determined by an interfacial energy balance [7]. However, it may be shown that the angle Φ of a grain corner in a stable quadrijunction must be greater than or equal to the angle ϕ of the same corner in the trijunction formed when the quadrijunction fluctuates into two trijunctions. If $\Phi < \phi$, as the trijunction moves incrementally away from the quadrijunction, the trijunction angle opens up, pulling the trijunction further from the quadrijunction, as shown in Fig. 1(a). If $\Phi \geqslant \phi$, as the trijunction moves incrementally away from the quadrijunction, the trijunction angle decreases and forces the trijunction back toward the quadrijunction, as shown in Fig. 1(b).

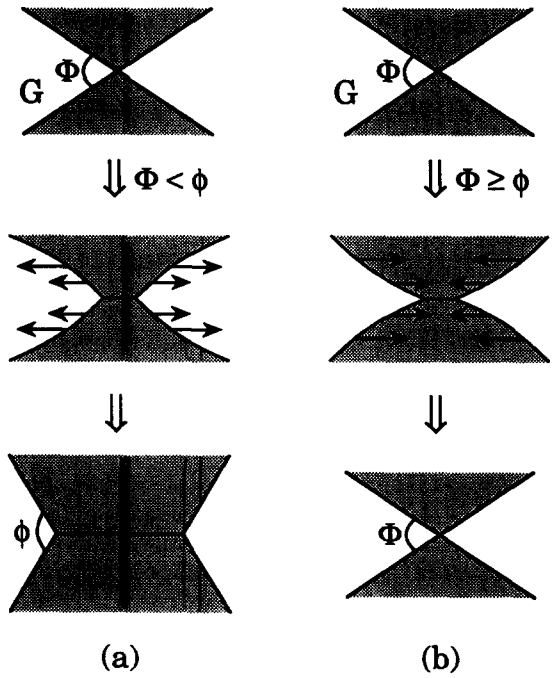

Fig. 1. Quadrijunction stability conditions dictate that the junction angle Φ of the (white) α grain G in the $\alpha\beta\alpha\beta$ quadrijunction be greater than the junction angle ϕ of the same grain in the $\alpha\beta\beta$ trijunction which forms when grain G fluctuates away from the quadrijunction. (a) If $\Phi < \phi$, the $\alpha\beta\beta$ trijunction opens up, pulling grain G away from the original quadrijunction position. (b) If $\Phi \geq \phi$, the $\alpha\beta\beta$ trijunction closes, pushing grain G back toward the original quadrijunction position. Arrows show the direction of the driving force for boundary motion in each case.

This criterion and the geometric fact that the angles around a quadrijunction must sum to 2π necessitate that only quadrijunctions of the $\alpha\beta\alpha\beta$ type are stable [4]. Since an $\alpha\beta\alpha\beta$ quadrijunction may fluctuate into two $\alpha\beta\beta$ trijunctions or into two $\alpha\alpha\beta$ trijunctions, such quadrijunctions are stable if and only if

$$\Phi_\alpha \geq \phi_\alpha \quad \text{and} \quad \Phi_\beta \geq \phi_\beta. \tag{6}$$

We can calculate an upper bound on the quadrijunction angles as well [4]. The balance of interfacial energies at the junction requires that the two α grain angles be the same and that the two β grain angles be the same. Then, since plane geometry requires that $2\Phi_\alpha + 2\Phi_\beta = 2\pi$, it is apparent that the maximum values of the quadrijunction angles are bounded such that

$$\Phi_\alpha \leq \pi - \phi_\beta \quad \text{and} \quad \Phi_\beta \leq \pi - \phi_\alpha. \tag{7}$$

Therefore, the ranges of stable quadrijunction angles are

$$\phi_\alpha \leq \Phi_\alpha \leq \pi - \phi_\beta \quad \text{and} \quad \phi_\beta \leq \Phi_\beta \leq \pi - \phi_\alpha. \tag{8}$$

These inequalities may be rewritten as a single quadrijunction stability criterion

$$\phi_\alpha + \phi_\beta \leq \pi \tag{9a}$$

which may be combined with trigonometric identities to give the equivalent expression [4]

$$R_\alpha^2 + R_\beta^2 \geq 4. \tag{9b}$$

It may be shown that junctions at which more than four grains meet are never stable in 2-D polycrystals [4].

The stability regimes of each of the microstructural features described above are shown in the $R_\alpha - R_\beta$ plane in Fig. 2(a) and in the $\phi_\alpha - \phi_\beta$ plane in Fig. 2(b). While Fig. 2 catalogs the thermodynamic stability regimes for all microstructural features, it does not predict the grain arrangements, phase distributions, or preferred microstructural features of a given system evolving via cooperative grain growth of many individual grains. In addition, the thermodynamic

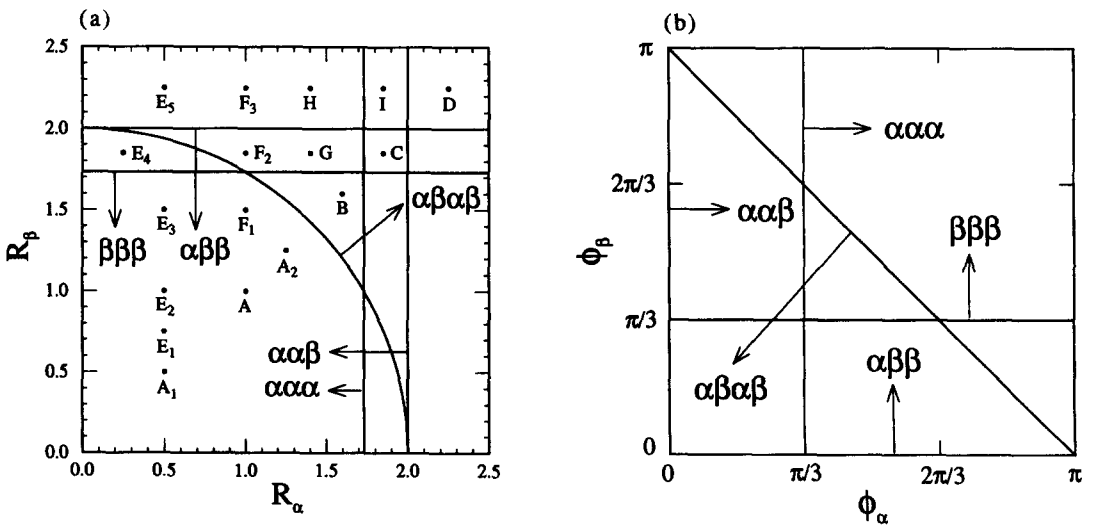

Fig. 2. Catalog of stable microstructural features in two phase systems. (a) The axes are the interfacial energy ratios $R_\alpha = \gamma_{\alpha\alpha}/\gamma_{\alpha\beta}$ and $R_\beta = \gamma_{\beta\beta}/\gamma_{\alpha\beta}$. Letters indicate conditions under which simulations were performed. (b) The same catalog plotted in terms of the interior angle of an α grain at an $\alpha\beta\beta$ trijunction, ϕ_α, and the interior angle of a β grain at an $\alpha\alpha\beta$ trijunction, ϕ_β.

analysis does not provide any information about boundary and interfacial energy effects upon the kinetics of microstructural evolution.

Laboratory experiments to test the effect of interfacial energies on two-phase microstructural evolution suffer from both conceptual and practical difficulties. For example, since interfacial energies in two-phase systems are determined by physical properties of the phases, a large number of different systems must be examined in order to reproduce the microstructural feature diagram of Fig. 2(a) over the range of R_α and R_β. Since each experimental system must be comprised of different phases, the kinetics of microstructural evolution are not directly comparable among the systems. Moreover, interfacial energy anisotropy differs from system to system. Finally, impurities and surface grooving often compete with curvature-driven grain growth in experiments on nominally 2-D systems (e.g. thin films). To circumvent the inherent difficulties of laborabory experiments, we employ a Monte Carlo Potts model computer simulation of 2-D, two-phase grain growth in which the only system variables are the three interfacial energies.

This paper summarizes a series of simulation results on one of the simplest cases of two-phase grain growth: the phase-volume nonconserved system (i.e. a system in which the volume fraction of each phase may vary during microstructural evolution). This type of system occurs during a congruent-point phase transition, defined as a transition from phase α to phase β, where α and β have identical bulk free energies and compositions. Alternatively, nonconserved domain evolution takes place when all distinct domains belong to one of two domain types. More often observed examples of "two-phase", phase-volume nonconserved growth occur during single phase grain growth when each grain belongs to one of two classes. For instance, in a highly textured system in which grains belong to one of two orientation classes, interfacial energies between like-orientation-class grains may be low relative to the interfacial energy between unlike-orientation-class grains. In systems undergoing recrystallization, dislocation cells belong to one class and grains to another, and boundaries between dislocation cells tend to be low-energy, low-angle boundaries, while boundaries between recrystallized grains and between recrystallized and non-recrystallized grains tend to be high-energy, high-angle. Similarly, during abnormal grain growth in a textured material, the interfacial energies between abnormally growing grains and between normally growing grains may be low compared to that between normal and abnormal grains. In all of these case, long-range diffusive processes play no part in microstructural evolution, and interfacial energies are the variables which affect the microstructural evolution of the polycrystal.

The computer experiments described below not only reproduce the microstructural feature diagram of Fig. 2, but also provide insight into the phase distributions, preferred microstructural features, and kinetics of two-phase microstructural evolution. In fact, these computer experiments demonstrate that the cooperative nature of grain growth in a polycrystalline system is critically important to both microstructural morphology and evolution.

2. SIMULATION METHOD

The Monte Carlo model for the simulation of normal grain growth has previously been described in theoretical and computational detail [11–18]. A continuum microstructure is mapped onto a 2-D, discrete lattice by assigning each lattice site a non-zero index, S_i. In the two-phase simulation, the sign of S_i indicates the phase present at that site; the absolute value of S_i corresponds to the orientation of the grain in which the site is embedded. Sites with one or more unlike nearest neighbors (i.e. sites located at a grain boundary or phase interface) are interface sites; sites with only like nearest neighbors are bulk (or interior) sites. The total system energy is specified by assigning a positive energy to interface sites and zero energy to interior sites, and is computed via the Hamiltonian

$$H = \frac{1}{8}\sum_{i=1}^{N}\sum_{j=1}^{z}\{(J_{\alpha\alpha}+J_{\beta\beta}+2J_{\alpha\beta})[1-\delta(S_i,S_j)] + (J_{\alpha\alpha}+J_{\beta\beta}-2J_{\alpha\beta})\mathrm{sgn}(S_i)\mathrm{sgn}(S_j) + (J_{\alpha\alpha}-J_{\beta\beta})[\mathrm{sgn}(S_i)+\mathrm{sgn}(S_j)]\} \quad (10)$$

where the outer sum is over all sites i, the inner sum is over the z nearest neighbors of site i, δ is the Kronecker delta function defined as $\delta(S_i, S_j) = 1$ if $S_i = S_j$ and 0 otherwise, sgn is the sign function defined as $\mathrm{sgn}(S_i) = 1$ if $S_i > 0$ and $\mathrm{sgn}(S_i) = -1$ if $S_i < 0$, and $J_{\alpha\alpha}$, $J_{\beta\beta}$ and $J_{\alpha\beta}$ are positive constants which scale with the α–α, β–β and α–β interfacial energies, respectively. In essence, this Hamiltonian sums interface energies; the system energy is simply $J_{\alpha\alpha}$ times the number of α–α boundary segments in the system plus $J_{\beta\beta}$ times the number of β–β segments plus $J_{\alpha\beta}$ times the number of α–β segments.

Initial grain structures are generated by assigning to each site i a random index S_i indicating both the phase and grain orientation of the site. (In these simulations, 50 different grain orientations were allowed in each phase, so $-50 \leqslant S_i \leqslant 50$ and $S_i \neq 0$.) Grain growth kinetics are determined through a Monte Carlo technique. First, a lattice site and a site index are chosen at random. The index of the chosen site is then changed to the new index if and only if the total system energy does not increase. Since only negative or zero energy excursions are allowed, the implicit Monte Carlo temperature of the simulation is $T = 0$. Note that because the boundary mobility remains finite, a Monte Carlo temperature of zero does not correspond to a physical temperature of 0 K; rather, setting the Monte Carlo temperature to zero simply eliminates thermal fluctuations in the

boundaries. After each attempted index change, time is incremented by $(1/N)$ Monte Carlo steps (MCS) where N is the number of lattice sites.

In the present simulations, lattice sizes of $N =$ 40,000 and 250,000 sites were employed. The microstructures were allowed to evolve for 10^5–10^7 MCS.

3. LATTICE EFFECTS

The validity of mapping a continuum microstructure onto a discrete lattice requires some justification. For instance, at a Monte Carlo temperature of zero, lattice effects are known to artificially pin grain growth on a square lattice with first nearest neighbor interactions [the sq(1) lattice], while grain growth on a triangular lattice with first nearest neighbor interactions [tri(1)] and grain growth on a square lattice with equal first and second neighbor interactions [sq(1, 2)] proceed to completion [15]. The factor which determines whether lattice effects may pin normal grain growth at $T = 0$ is the ability of grain junctions to maintain their equilibrium angles independent of lattice orientation [16]; an energetically anisotropic lattice will tend to force grain junctions to low lattice-energy angles which are far from the junction equilibrium angles.

Lattice anisotropy becomes even more important in two-phase grain growth, where not only must $\alpha\alpha\beta$ and $\alpha\beta\beta$ grain junctions maintain different equilibrium angles, but also, in some cases, nucleation of an unlike phase grain may occur at $\alpha\alpha\alpha$ or $\beta\beta\beta$ trijunctions. Consider for example, a $\beta\beta\beta$ trijunction in a system with $R_\alpha = 1.4$ and $R_\beta = 1.85$. Thermodynamically, an α grain should nucleate at the trijunction (see Fig. 2 and Ref. [4]). However, in both the tri(1) and sq(1, 2) lattices, there are $\beta\beta\beta$ trijunction configurations which are stable and do not permit α nucleation. When grain growth occurs on these lattices, the disappearance of kinks on the grain boundaries causes the evolved microstructures to contain the artificially stable trijunctions as well as other remnants of the lattice geometry. For example, in a system with $R_\alpha = 1.4$ and $R_\beta = 1.85$, the tri(1) microstructure in Fig. 3(a) contains artificially stable $\beta\beta\beta$ trijunctions and many triangular grains; the sq(1, 2) microstructure in Fig. 3(b) includes artificially stable $\beta\beta\beta$ trijunctions and square grains. In addition, both of these systems stop evolving at a relatively small grain size.

These lattice effects are caused by the energetic anisotropy of the lattices. While in a single phase system every lattice site reorientation attempt incurs an energy change which is an integer multiple of the energy scaling factor $J_{\alpha\alpha}$, during two phase grain growth the system must respond isotropically to energy changes which may be a small fraction of $J_{\alpha\alpha}$. The Wulff plot of bond energy vs lattice orientation for the tri(1) lattice is hexagonal and contains minima which are 13% lower in energy that the energy maxima located $\pi/6$ from the minima; likewise, the octagonal Wulff plot for the sq(1, 2) lattice has minima which are 10% lower in energy than its maxima [19]. These lattice energy minima must not overwhelm the true, continuum interfacial energy minima in the system, so in order to maximize the energetic sensitivity of the lattice, we choose a lattice with very small energetic anisotropy. In this case, the triangular lattice with equal first and second nearest neighbor interactions [the tri(1, 2) lattice], which exhibits only a 5% energetic anisotropy in its dodecagonal Wulff plot, was found to be sufficiently sensitive. For the test case of $R_\alpha = 1.4$ and $R_\beta = 1.85$, the tri(1, 2) system contains no artificially stable $\beta\beta\beta$ trijunctions, and the grain shapes do not mimic the underlying triangular lattice, as shown in Fig. 3(c). Finally, note that since the Wulff shapes of these growth lattices are polygonal, the driving force for boundary motion in the simulations is crystalline weighted mean curvature, as discussed by Taylor [5], and boundaries have an arbitrary minimum facet size which depends upon the lattice size.

4. MICROSTRUCTURES

The Monte Carlo computer simulation on the tri(1, 2) lattice, described above, was applied to two-phase, congruent-point grain growth over a large range of R_α and R_β values (at each point indicated by a capital letter in Fig. 2). The resultant microstructures are analyzed below.

4.1. $R_\alpha = R_\beta$ diagonal feature fields

Along the diagonal of the R_α–R_β microstructural feature diagram (Fig. 2), α–α and β–β grain boundary energies are equivalent, so α and β grains should possess identical microstructural features and area fractions. The single parameter which influences grain structure and distribution when $\gamma_{\alpha\alpha} = \gamma_{\beta\beta}$ is the α–β interfacial energy $\gamma_{\alpha\beta}$. The progression of microstructures along the diagonal of the R_α–R_β microstructural feature diagram show the transition from the "normal" grain growth regime where only trijunctions are energetically stable ($\gamma_{\alpha\alpha} = \gamma_{\beta\beta} < \sqrt{2}\gamma_{\alpha\beta}$) to the wetting regime where quadrijunctions alone are stable ($\gamma_{\alpha\alpha} = \gamma_{\beta\beta} > 2\gamma_{\alpha\beta}$).

The simplest case of two-phase, congruent-point grain growth is the situation where $\gamma_{\alpha\alpha} = \gamma_{\beta\beta} = \gamma_{\alpha\beta}$ or $R_\alpha = R_\beta = 1$ (point A in Fig. 2). Since the interfacial energies in the system are equal and isotropic, and the free energies of the phases are equivalent, this situation should correspond to normal grain growth with a random distribution of α and β grains. Figure 4(a) shows a typical microstructure in this system; grain shapes are spatially isotropic, there is no discernable difference between α and β grains, and the only junctions present are the expected $\alpha\alpha\alpha$, $\beta\beta\beta$, $\alpha\alpha\beta$ and $\alpha\beta\beta$ trijunctions. In addition, the area fractions of α and β are approximately 0.5 until late times, when random fluctuations may cause either phase to

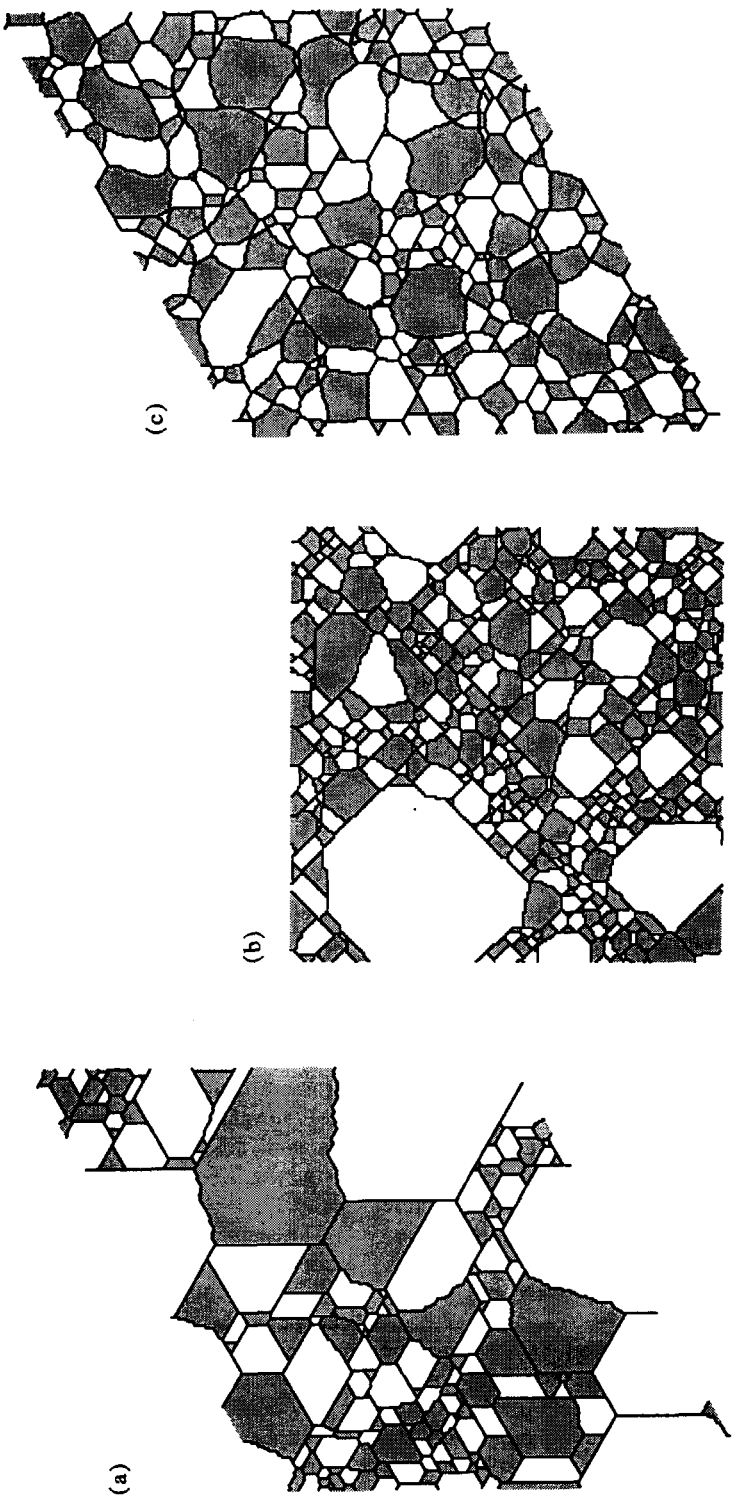

Fig. 3. The effect of lattice anisotropy on microstructure in simulated system G. Grains of phase α are white; β grains are gray. (a) The tri(1) lattice gives artificially stable $\beta\beta\beta$ trijunctions and many triangular grains. (b) The sq(1, 2) lattice gives artificially stable $\beta\beta\beta$ trijunctions and square grains. (c) The tri (1, 2) system contains no artificially stable features, and grain shapes do not mimic the lattice symmetry.

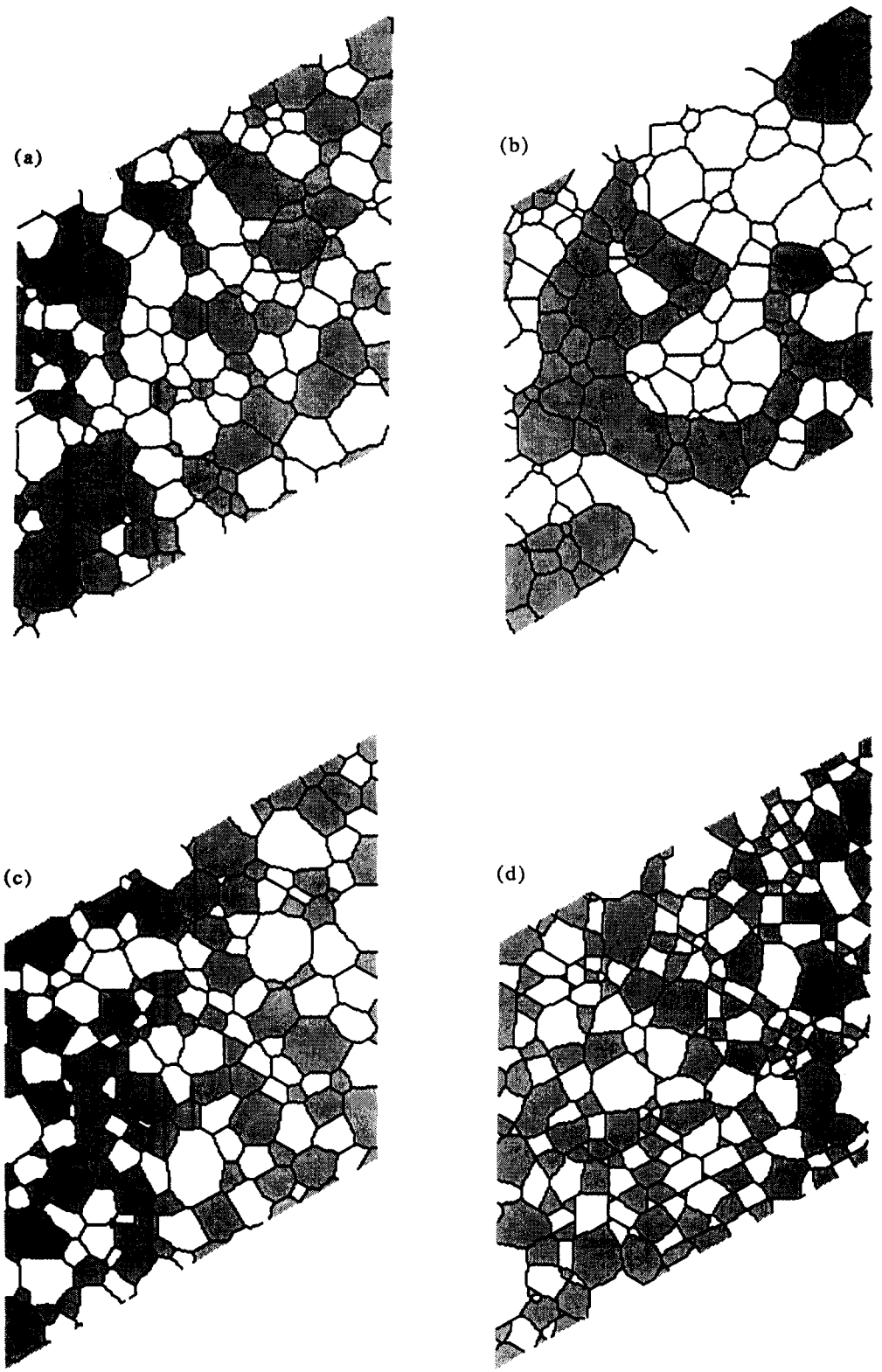

Fig. 4. (a–d) *Caption overleaf.*

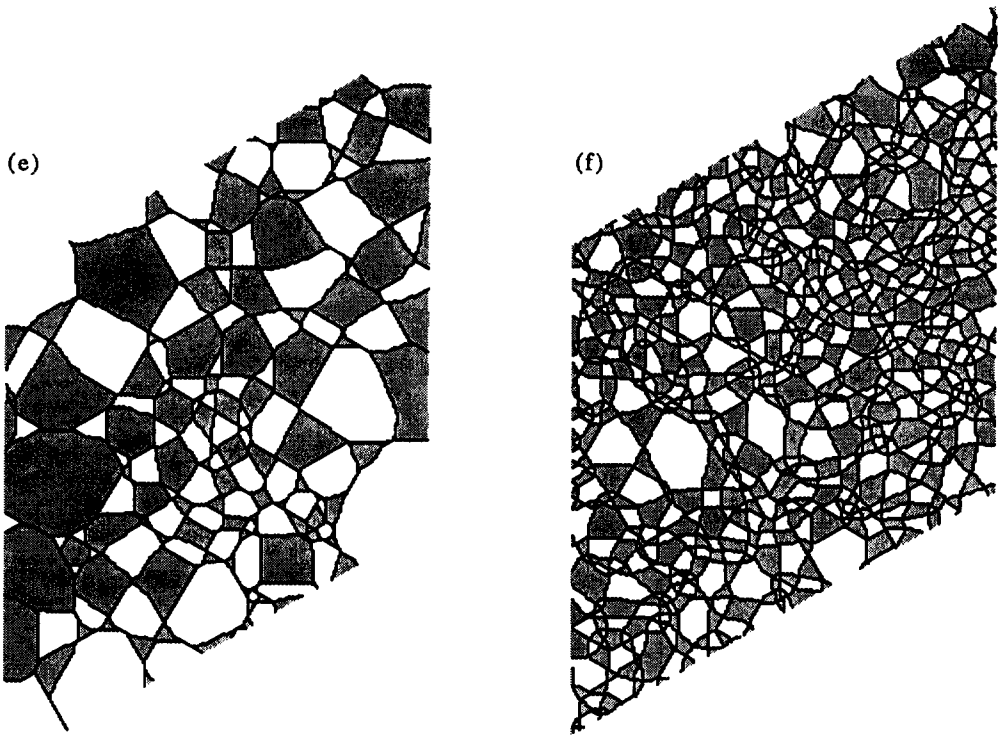

Fig. 4. Microstructures of two-phase systems with $R_\alpha = R_\beta$. Grains of phase α are white; β grains are gray. (a) Normal grain growth in system A. (b) Phase clustering in system A_1. Note that grains within phase clusters grow almost as if in isolation. (c) Alternating phases in system A_2. (d) All microstructural features are stable in system B; however, since phases have a tendency to alternate, $\alpha\alpha\alpha$ and $\beta\beta\beta$ trijunctions are present only in small numbers. (e) $\alpha\alpha\alpha$ and $\beta\beta\beta$ trijunctions disappear in system C. (f) Double wetting in system D; phases alternate perfectly and all junctions are quadrijunctions. Grain structures (e) and (f) consist solely of very low curvature grains and are pinned.

dominate as the system approaches a single grain, as shown in Fig. 5.

For a system with $R_\alpha = R_\beta < 1$, all trijunctions are stable, as in normal grain growth. However, in this case, the α–β interfacial energy is greater than either grain boundary energy, so the system will evolve to minimize α–β interfaces. For instance, for $R_\alpha = R_\beta = 0.5$ (point A_1 in Fig. 2), Fig. 4(b) shows a typical microstructure, characterized by continuous, smooth clusters of α grains and β grains. These clusters are compact, and grain growth within the clusters occurs almost as if the grains grow in isolation. (Note the bamboo-like grain structure of the straight grain boundaries along "channels" of α and β.) Figure 5 shows that the volume fraction of each phase differs from 0.5 even at very early times. This effect is geometric, not energetic. The percolation threshold for a two-phase continuum is 0.5, so if one phase randomly achieves a volume fraction slightly greater than 0.5, it will completely surround the other (non-percolating) phase, and thus will always grow at the expense of the non-percolating phase. Therefore, in simulations with random initial grain configurations, half of the independent trials evolve toward an all-α state, and the other half approach an all-β state.

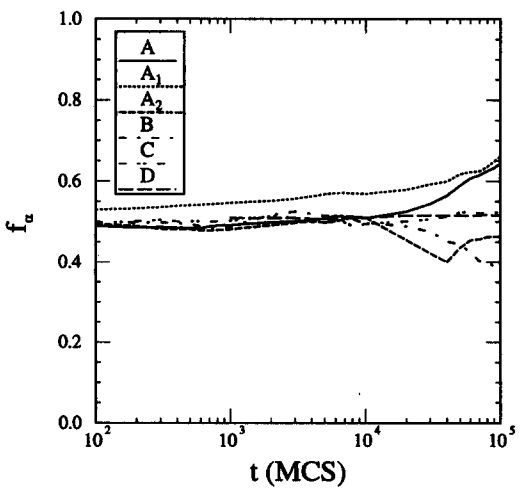

Fig. 5. The time evolution of the volume fraction of phase α, f_α, in on-diagonal, two-phase systems A, A_1, A_2, B, C and D.

In contrast, the system with $R_\alpha = R_\beta > 1$ favors maximizing the amount of α–β interface present in the microstructure. For $R_\alpha = R_\beta = 1.25$ (point A_2 in Fig. 2), the microstructure is characterized by α and β grains which alternate more than in the normal growth case, as shown in Fig. 4(c). In other words, an α grain is more likely to have β neighbors than α neighbors. In this system, the volume fraction of

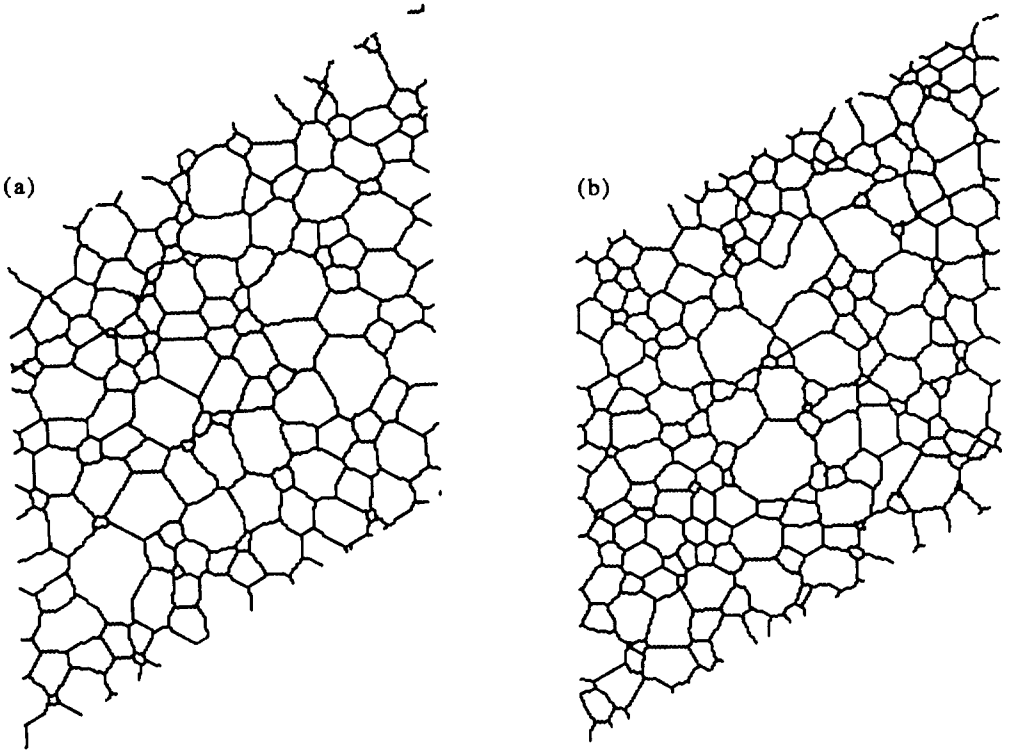

Fig. 6. Single phase microstructures produced by an interfacial energy induced phase transition to phase α (shown in white). (a) All trijunctions are thermodynamically stable in system E_2. (b) Quadrijunctions are thermodynamically stable in system E_5. However, due to the phase transition, the only observed grain junction in either system is the $\alpha\alpha\alpha$ trijunction.

both phases remains near 0.5 until very late times (see Fig. 5).

Continuing up the $R_\alpha = R_\beta$ diagonal, α–α and β–β boundaries become relatively more energetic compared to α–β interfaces, and the phases are more inclined to alternate, until at $R_\alpha = R_\beta = \sqrt{2}$, $\alpha\beta\alpha\beta$ quadrijunctions become stable. For the system with $R_\alpha = R_\beta = 1.6$ (point B in Fig. 2), the microstructure contains these quadrijunctions as well as $\alpha\alpha\beta$ and $\alpha\beta\beta$ trijunctions, as shown in Fig. 4(d). The thermodynamically stable $\alpha\alpha\alpha$ and $\beta\beta\beta$ trijunctions are also present, but since the phases have a strong tendency to alternate in order to maximize the low energy α–β interface at the expense of the higher energy α–α and β–β interfaces, these same-phase trijunctions (which require the intersection of three α–α or three β–β interfaces) are present in very small numbers.

For $R_\alpha = R_\beta > \sqrt{3}$, high α–α and β–β boundary energies destabilize the $\alpha\alpha\alpha$ and $\beta\beta\beta$ trijunctions. Microstructures of the system with $R_\alpha = R_\beta = 1.85$ (point C in Fig. 2), shown in Fig. 4(e), consist of $\alpha\alpha\beta$ and $\alpha\beta\beta$ trijunctions and $\alpha\beta\alpha\beta$ quadrijunctions exclusively. As discussed below, the structure eventually becomes pinned in a checkerboard configuration containing mainly $\alpha\beta\alpha\beta$ quadrijunctions and a small number of $\alpha\alpha\beta$ and $\alpha\beta\beta$ trijunctions. As in the other cases on the R_α–R_β diagonal, the area fractions of α and β are 0.5, and the cessation of microstructural evolution prevents one phase from dominating at late times, as shown in Fig. 5.

In the on-diagonal wetting regime with $R_\alpha = R_\beta > 2$, the only stable microstructural features are $\alpha\beta\alpha\beta$ quadrijunctions and α–β interfaces. Accordingly, the evolved microstructure of the system with $R_\alpha = R_\beta = 2.25$ (point D in Fig. 2) contains only these features, as shown in Fig. 4(f); phases alternate so that α is surrounded entirely by β and vice versa. The volume fractions of α and β are quickly pinned at 0.5.

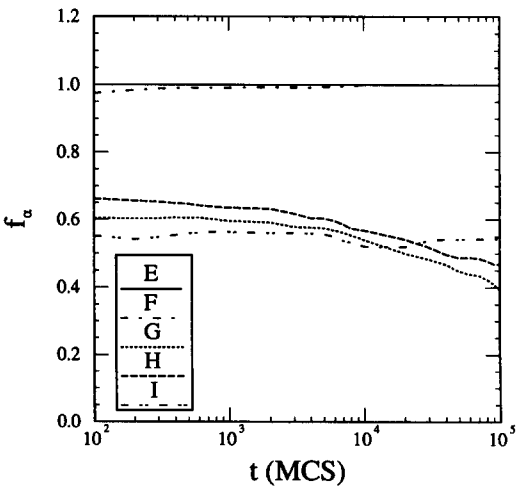

Fig. 7. The time evolution of the volume fraction of phase α, f_α, in off-diagonal, two-phase systems E, F, G, H and I.

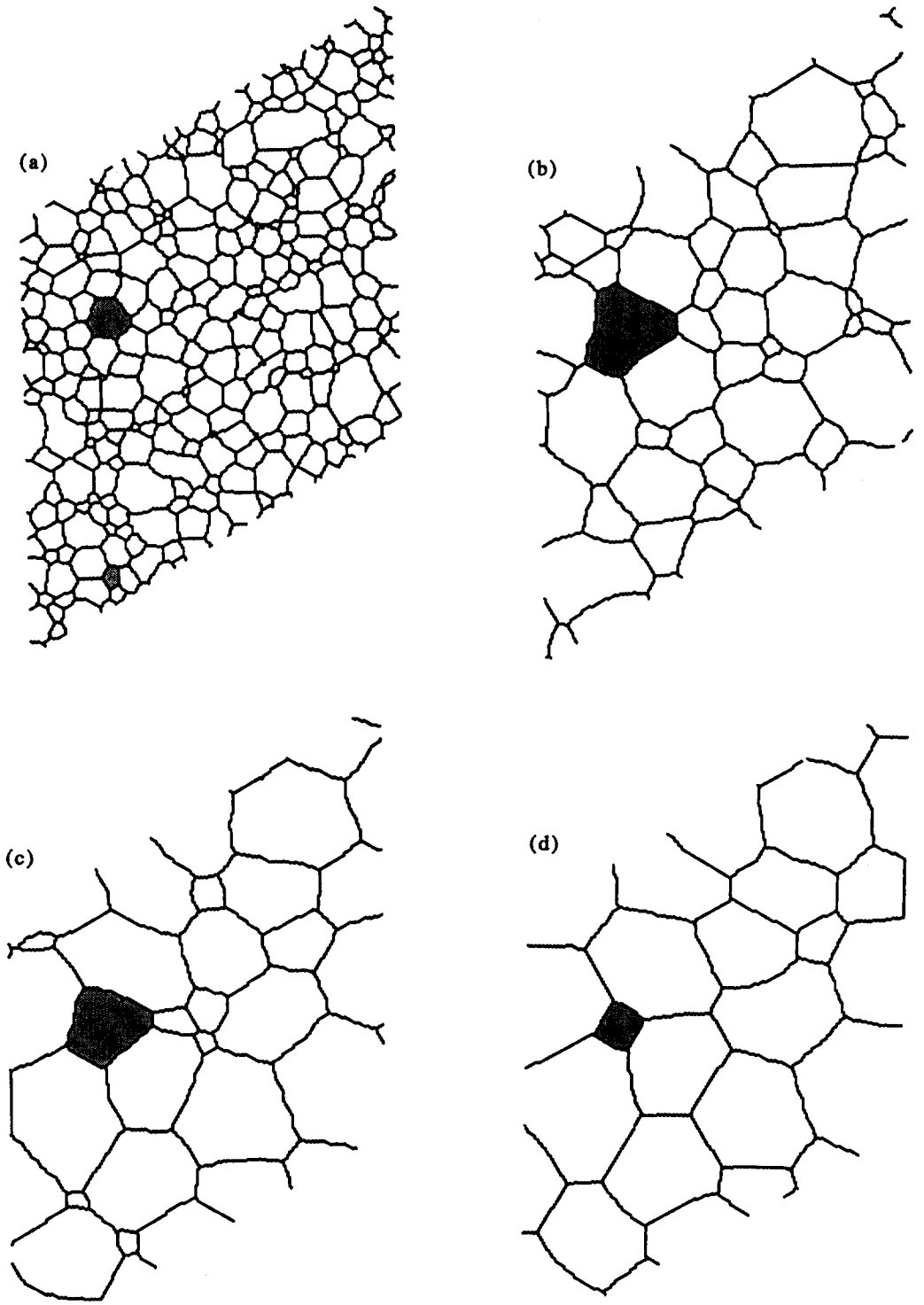

Fig. 8. Microstructural evolution in system F_1, which favors isolated grains of β (gray) in an α (white) matrix. Isolated β grains follow the "six minus n" growth rule. For instance, the β grain in the upper left corner (a) grows when $n = 7$, (b) stabilizes when $n = 6$, and (c) shrinks when $n = 5$ and (d) $n = 4$.

4.2. Off-diagonal feature fields

In the off-diagonal regimes of the R_α–R_β diagram, the difference between α–α and β–β grain boundary energies adds phase asymmetry to the already complex geometric and energetic constraints upon the system.

In the regime where $R_\alpha < R_\beta$ and $R_\alpha < 1$, α–α grain boundaries have lower energy than either β–β boundaries or α–β interfaces. Hence, the system

should evolve to maximize the length of α–α grain boundaries. In fact, a system with $R_\alpha = 0.5$ and $R_\beta = 1$ (point E_2 in Fig. 2) evolves to contain only low energy α–α boundaries, and the volume fraction of α is unity following a short transient, as shown in the microstructure in Fig. 6(a) and in Fig. 7. This is an excellent example of a phase transition that is controlled by interfacial energy; although the free energies of α and β are identical, α is the thermodynamically stable phase in a polycrystalline system because an all-α system minimizes the interfacial energy of the system. An exactly analogous situation occurs in systems E_1, E_3, E_4 and E_5 in Fig. 2; since α–α grain boundaries have the lowest interfacial energy, each system evolves to contain only α grains in a normal grain structure regardless of the microstructural features thermodynamically accessible to it. In fact, even in systems where β wets α–α interfaces (i.e. $R_\alpha > 2$), the microstructure remains a normal, all-α microstructure, as shown for system E_4 in Fig. 6(b). Once all β has been eliminated from such a system, normal single-phase grain growth occurs.

In the regime where $R_\alpha < R_\beta$ and $R_\alpha = 1$, α–α grain boundaries have the same energy as α–β interfaces, and both have lower energies than β–β grain boundaries. In this case, the system equally favors isolated β grains in an α matrix or an all-α system. Three examples of such a system are points F_1, F_2 and F_3 in Fig. 2. Because α grains may grow whether in contact with α or β grains and β grains may only grow when surrounded by α grains, α grains quickly surround β grains. However, since all corners of a β grain surrounded by α grains have interior angles of $2\pi/3$, once isolated, a β grain grows (or shrinks) normally among its α neighbors; that is, an isolated β grain follows the "six minus n" growth rule. Microstructural evolution in such a system is shown in Fig. 8. Note that if an isolated β grain has fewer than 6 sides (as most eventually do) it shrinks and disappears. However, if a β grain has more than 6 sides [as the large β grain in the upper left corner of Fig. 8(a)], it grows. Because the vast majority of grains eventually disappear during normal grain growth, very few of these normally evolving β grains remain at late times; thus, the volume fraction of α approaches 1. For example, the large, growing β grain in Fig. 8(a) eventually loses neighbors until fewer than six remain; then, it shrinks and disappears, as shown in Fig. 8(b–d). Note, however, that there is a small, finite probability that an isolated β grain will be the single grain that remains when all others have disappeared. In that unlikely case, the volume fraction of β might actually approach unity at very late times.

In the regime where $R_\alpha < R_\beta$ and $R_\alpha > 1$, the α–β interface is of lower energy than any other interface in the system, and α and β grains tend to alternate. Because the total lengths of α–α and β–β interfaces are minimized by grain alternation, the relative magnitudes of $\gamma_{\alpha\alpha}$ and $\gamma_{\beta\beta}$ have very little effect upon the phase distribution of the system. In fact, the volume fractions of each phase are about equal, and all stable microstructural features are present. Hence, the microstructures closely resemble those of the on-diagonal systems containing the same stable features as the off-diagonal system.

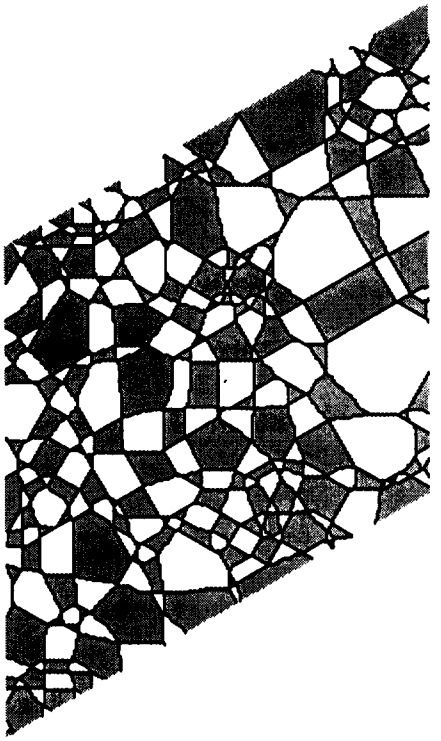

Fig. 9. Alternating phases in system I. Grains of phase α are white; β grains are gray. Note the similarity to the system C microstructure [Fig. 4(e)]; the two systems differ only in the stability of $\alpha\beta\beta$ trijunctions.

For example, if $\sqrt{3} < R_\beta < 2$, $R_\alpha < \sqrt{3}$, and $R_\alpha^2 + R_\beta^2 > 4$, all features except $\beta\beta\beta$ trijunctions are thermodynamically allowed. As shown in Fig. 3(c), an evolved structure for the system $R_\alpha = 1.4$ and $R_\beta = 1.85$ (point G in Fig. 2) contains only stable features in a microstructure very similar to the $R_\alpha = R_\beta = 1.6$ case in Fig. 4(d). This might be expected, since the stable features of the $R_\alpha = 1.4$, $R_\beta = 1.85$ system differ from those of the $R_\alpha = R_\beta = 1.6$ system only in the instability of $\beta\beta\beta$ trijunctions, which occur very infrequently in the $R_\alpha = R_\beta = 1.6$ system. The volume fraction of α and β become pinned near 0.5 (see Fig. 7).

Likewise, for $\sqrt{3} < R_\alpha < 2$, $R_\beta > 2$, only $\alpha\alpha\beta$ trijunctions and $\alpha\beta\alpha\beta$ quadrijunctions are stable. As shown in Fig. 9, an evolved structure for the system $R_\alpha = 1.85$ and $R_\beta = 2.25$ (point I in Fig. 2) contains only stable features in a microstructure very similar to the $R_\alpha = R_\beta = 1.85$ case in Fig. 4(e). This might be expected, since the stable features of the $R_\alpha = 1.85$, $R_\beta = 2.25$ system differ from those of the $R_\alpha = R_\beta = 1.85$ system only in the instability of $\alpha\beta\beta$ trijunctions. Since the most common grain junction in these

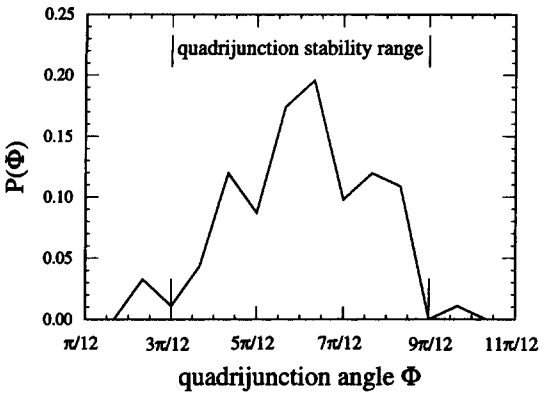

Fig. 10. Quadrijunction angles in a system C microstructure in which $\phi_\alpha = \phi_\beta \cong \pi/4$. Quadrijunction stability criteria require all quadrijunction angles Φ be greater than $3\pi/12$ but less than $9\pi/12$.

systems is the quadrijunction, the presence or absence of $\alpha\beta\beta$ trijunctions affects the appearance of the microstructures very little. As in the $R_\alpha = R_\beta = 1.85$ system, the microstructure eventually becomes pinned, which causes the volume fraction of α and β to remain near 0.5 at all times (Fig. 7).

4.3. Quadrijunction angles

Recall that according to equation (8), $\alpha\beta\alpha\beta$ quadrijunctions are stable when quadrijunction angles Φ_α and Φ_β are within the ranges $\phi_\alpha \leqslant \Phi_\alpha \leqslant \pi - \phi_\beta$ and $\phi_\beta \leqslant \Phi_\beta \leqslant \pi - \phi_\alpha$. Figure 10 shows measured α and β grain quadrijunction angles in a simulated microstructure in which $R_\alpha = R_\beta = 1.85$ and $\phi_\alpha = \phi_\beta \cong \pi/4$ [system C in Fig. 2 and the microstructure in Fig. 4(e)]. In this system, equation (8) requires all quadrijunction angles Φ to be greater than $3\pi/12$ but less than $9\pi/12$. Indeed, the distribution of quadrijunction angles falls almost entirely with the limits given by equation (8) and is peaked at the center of the stability range (i.e. at about $6\pi/12$). A very few quadrijunction angles fall outside of the stable range (about 3% have an angle of about $2\pi/12$ and 1% have an angle of about $10\pi/12$). Because there are so few unstable angles, it is possible that they occur during a transient configuration of a forming, decomposing, or moving quadrijunction. Additionally, the anisotropy of the tri(1, 2) lattice makes it slightly more energetically favored for boundaries or interfaces to intersect one another at an angle of $2\pi/12$ than at $3\pi/12$ and at $10\pi/12$ rather than $9\pi/12$. The slight depressions in the quadrijunction angle distribution at $5\pi/12$ and $7\pi/12$, also less favored intersection angles, tends to corroborate the possibility of lattice effects upon quadrijunction angles.

5. PHASE AND FEATURE DIAGRAMS

During microstructural evolution from an initially random system, the effects of cooperative grain growth and the assumption of a phase-volume nonconserved system strongly influence grain arrangement, phase

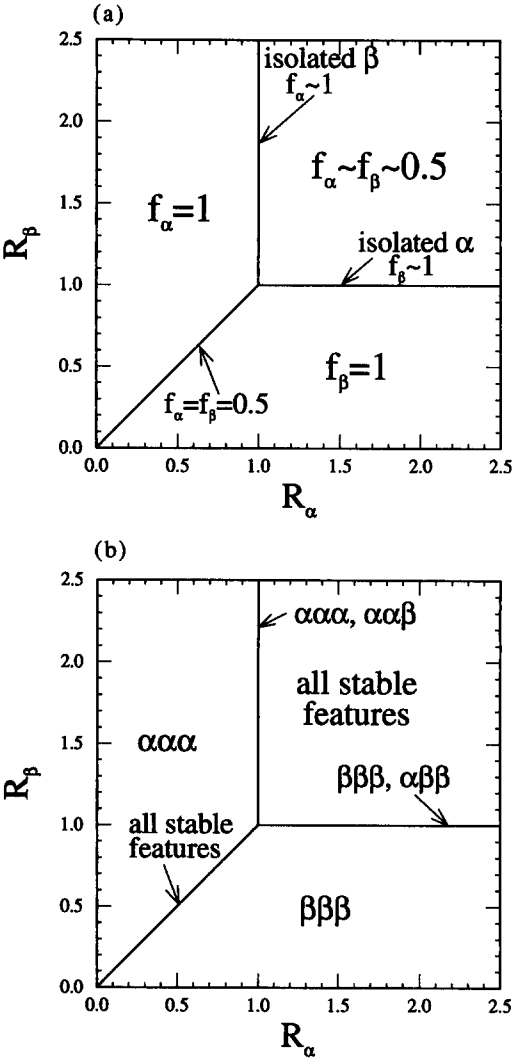

Fig. 11. The effects of interfacial energy ratios on a two-phase polycrystal in which phase volumes are not conserved. (a) The phase diagram of the system. The interfacial energy ratios R_α and R_β control the phases present in the system. (b) Microstructural features in the system. Although Fig. 2 may indicate that a number of features are stable, the condition that phase volume is not conserved may effectively eliminate certain features from the microstructure.

distribution, and preferred microstructural features. For instance, since the bulk free energy of α and β are equivalent, grain boundary and interfacial energies control the phases present in the system. Thus, a phase diagram for the α–β system may be plotted in the R_α–R_β plane, as shown in Fig. 11(a). Four distinct phase fields occur. In an infinite system, along the $R_\alpha = R_\beta$ diagonal each phase has a volume fraction of exactly 0.5, while in the off-diagonal regime where $R_\alpha > 1$ and $R_\beta > 1$, the phase volume fractions only approximate 0.5. Similarly, along the isolated grain lines, the phase fraction of the majority phase is close to unity, while in the interfacial energy induced phase transition regime, the volume fraction of the favored phase goes to exactly 1.

The microstructural features present in a phase-volume nonconserved system are also functions of R_α and R_β, as shown in Fig. 11(b). When the volume fractions of α and β are not nearly equal, some thermodynamically permitted features may never appear in evolving polycrystals. For instance, single phase systems may contain only same-phase trijunctions no matter which other features are thermodynamically stable. Likewise, in isolated grain systems, only one same-phase and one two-phase trijunction ever occur. However, when the phase volume fractions of α and β are essentially equal, all thermodynamically stable features are observed throughout microstructural evolution.

Together with the microstructural feature stability diagram of Fig. 2, Fig. 11(a,b) provides a complete description of the phases and features present in a polycrystalline, two-phase microstructure in which phase volume is not conserved during microstructural evolution.

6. KINETICS AND MICROSTRUCTURAL FEATURES

6.1. Trijunction-only systems

The grain size evolution kinetics for systems containing only trijunctions (i.e. all A, E, and F systems) are shown in Fig. 12. Such systems undergo normal grain growth (average grain area $\langle A \rangle$ proportional to t^m where m is asymptotic to one at late times [17]) with late-time kinetics very similar to those of single phase systems.

As shown in Fig. 12, trijunction-only systems in which $f_\alpha \sim 1$ at late times (i.e. all E and F systems) show slightly depressed grain growth kinetics at early times. This initial transient is due to the disappearance of β grains. At early times, α grains grow at the expense of β grains. So while the α grains maintain their single phase grain growth dimensions, the β grains are all much smaller than in normal grain growth, and the mean grain size is depressed relative to the single phase case. At later times, when $f_\beta \sim 0$, the α grains (and isolated β grains, if any) are at the size they would have been if no shrinking β grains had ever been present, and the structure continues to grow normally. Hence, phase transition (E) and isolated β systems (F) display slow initial grain growth kinetics which accelerate and catch up to those for the single phase systems at late times.

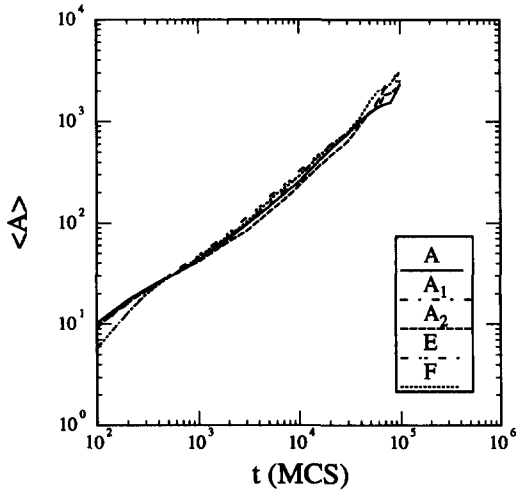

Fig. 12. The evolution of mean grain area $\langle A \rangle$ in systems containing only trijunctions. Late-time kinetics are very similar to normal, single-phase growth kinetics.

For trijunction-only systems in which α and β are present in approximately equal quantities (points A, A_1 and A_2 in Fig. 2), grain size evolution kinetics are very similar to the single phase case at all times (Fig. 12). This is a consequence of the independence of the grain growth kinetics from grain geometry. In particular, Mullins and Viñals have shown that normal grain growth kinetics (i.e. $\langle A \rangle = kt$) are required when the grain size and topological distributions are self-similar during grain evolution; the time prefactor k in the normal growth equation is determined by the shapes of the size and topology distributions [20]. Since the experimentally observed grain size and topology distributions are self-similar after initial transients ($t > 1000$ MCS) in all trijunction-only systems, these systems must follow normal grain growth kinetics.

Moreover, if the topology and grain area distributions of two trijunction-only systems are the same, the growth kinetics of the systems must be identical as well. While such similarity between trijunction-only systems is not a necessity, grain area distributions are found to be statistically equivalent in the three systems studied. Grain topology distributions for these systems vary slightly and are shown in Fig. 13. The alternating phase case A_2 differs most from the single phase grain topology (case A) with a peak at $n = 6$ neighbors rather than $n = 5$, and indeed, the time prefactor is smaller and kinetics are depressed relative to case A (Fig. 12). The grain clustering system A_1 has grain topology essentially equivalent to the single phase case, and its kinetics

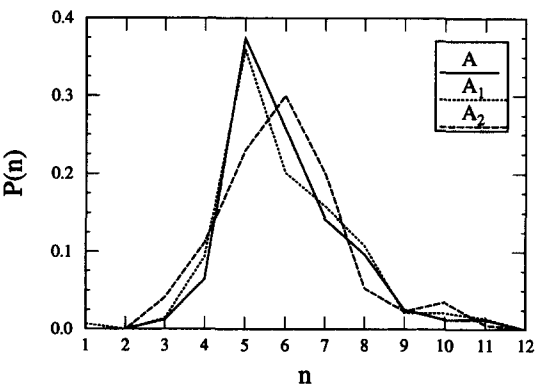

Fig. 13. Distribution of grain topology in trijunction-only systems. Note that the phase clustering system (A_1) is very similar to the single-phase system (A), while the alternating phase system (A_2) has a broader, more symmetrical distribution of grain shapes.

are nearly identical to the single phase kinetics. Therefore, the degree of similarity in grain evolution kinetics between trijunction-only systems is associated with topological similarity, regardless of the respective geometries of the systems. This observation re-emphasizes the governing role of topology in grain growth in polycrystals, elucidated by Smith 40 years ago [1].

Besides controlling the rate of grain evolution, topology also governs the persistence of grain growth. In a single phase system with trijunction angles of $2\pi/3$, the only non-evolving grain structure is the topologically ordered hexagonal array of grains. However, a topologically disordered system does not evolve toward the hexagonal system (either for energetic or kinetic reasons). For instance, a 6-sided grain is locally stable but does not offer resistance to topological perturbations; that is, the 6-sided grain does not inhibit its neighbors from either growing or shrinking away. So during grain growth from a disordered initial system, clusters of hexagonal grains are not particularly favored to form or to persist. In fact, even an infinite hexagonal array of grains is unstable with respect to a single 5–7 topological perturbation [21, 22].

The topology of a trijunction-only grain in a two-phase system is fully described by three parameters: the number of corners n, the number of unlike-phase neighbor grains n_d, and the number of switches from α to β as we examine the neighbor grains in clockwise order n_s. The values which these parameters may take are limited by a set of inequalities and may be determined by linear programming [4]. The integrated curvature of a trijunction-only, α grain G_α is given by

$$\int_{G_\alpha} \kappa \, ds = (\pi/3) \cdot (6 - n) + (\phi_\alpha - 2\pi/3) \cdot (n_d - n_s) - (\phi_\beta - 2\pi/3) \cdot n_s \quad (11)$$

(for a β grain, switch the α and β subscripts) [4]. A grain with zero integrated curvature is termed a ZIC grain. Since the change in area of a grain is proportional to its integrated curvature by equation (4), a ZIC grain is kinetically stable and will neither grow nor shrink. A structure comprised solely of ZIC grains (as the single phase hexagonal array of grains) has no driving force for microstructural evolution. Even though the lowest energy configuration for the system is a single crystal, an array of ZIC grains is metastable and will persist. Conversely, a structure containing even a few non-ZIC grains must evolve.

The 6-sided grain surrounded by like-phase neighbors is a ZIC grain in any system; however, in a two-phase, all-ZIC system, some ZIC grains must have unlike-phase neighbors. Equation (11) shows that ZIC grains with $n_d \neq 0$ can form only along certain lines in the $\phi_\alpha - \phi_\beta$ plane [Fig. 2(b)]. For instance, 4-sided ZIC grains occur for (n, n_d, n_s) of (4,4,0), (4,3,1), (4,2,1) and (4,2,2); setting equation (11) to zero and inserting these parameters generates the set of stability lines for 4-sided grains [i.e. the (4,3,1) grain is a ZIC grain if $\phi_\alpha = \phi_\beta/2$].

Even in systems which permit ZIC grains, topological or geometric constraints may prohibit an all-ZIC grain structure from forming. For example, in a trijunction only system, the Euler–Poincare relation requires that the average number of edges per grain $\langle n \rangle$ equal 6; thus, any all-ZIC grain structure must have some ZIC grains of $n \leqslant 6$ present. In the trijunction-only energetic regime, there are only 26 types of ZIC grains with $n \leqslant 6$; any system with interfacial energetics that do not fall upon one of those 26 ZIC lines can never form a kinetically stable structure of ZIC grains, and grain growth must persist.

It may be shown by writing equation (11) for α and β grains and setting both expressions to zero that for any system which allows some ZIC grains of phase α with $n(\alpha) \leqslant 6$, some β grain with $n(\beta) = 12 - n(\alpha)$ is stable as well. While this would seem to imply that a structure comprised of half α grains with $n(\alpha)$ sides and half β grains with $n(\beta)$ sides is stable, there is no guarantee that the geometry of these ZIC grains permits such a structure to tile 2-D space. So even when the Euler–Poincare relationship is satisfied, a space-filling, all-ZIC grain structure may not form.

Finally, in the trijunction-only two-phase systems which can form tilings of ZIC grains, there is no clear driving force to form the all-ZIC grain structure. Because trijunction angles are thermodynamically fixed, the junctions of a ZIC grain can only adjust to changes in neighbor grain shape or arrangement by moving, and since junction angular constraints are thermodynamic boundary conditions, junction motion proceeds freely. Therefore, in the two-phase, trijunction-only system, just as in the single-phase system, a ZIC grain does not offer resistance to perturbations in its number or arrangement of neighbors. So during grain growth from a disordered initial system, clusters of properly tiled, ZIC grains are not particularly favored to form or to persist. In fact, the complexity of tiling phases as well as shapes ensures that large ZIC clusters will form from a random initial configuration with essentially zero probability.

Therefore, in any system in which all grain junction angles are fixed, grain growth must occur and persist.

6.2. Quadrijunction systems

In 1952, Smith wrote, "Quite contrary to Harker and Parker [23], [this] writer predicts that grain growth will slow and stop (in the absence of inclusions) only when grain corner angles can *depart* from 120 degrees instead of when they *approach* it . . ." [1]. On the basis of the above discussion, we may generalize Smith's statement to multiphase systems: grain growth cannot cease (in the absence of inclusions) when grain junction angles are thermodynamically fixed.

However, recall that quadrijunction angles are not thermodynamically fixed; equation (8) shows that quadrijunctions are stable over a range of junction

angles. Can grain growth cease in a system in which grain junction angles may vary?

The topology of any grain in a two-phase system is fully described by four parameters: n, n_d, n_s, and the number of quadrijunction corners n_q. (Note that neighbors are now defined as grains with which the grain of interest shares an edge.) The integrated curvature of an α grain with topological characteristics (n, n_d, n_s, n_q) is given by

$$-\int_{G_\alpha} \kappa \, ds = (\pi/3)\cdot(n - 4n_s + 2n_d) + \phi_\beta \cdot n_s - (\phi_\alpha)\cdot(n_d - n_s - n_q) - \sum_{n_q} \Phi_\alpha - 2\pi \quad (12)$$

where Φ_α are the n_q quadrijunction angles, which may all be different [4]. In fact, since each Φ_α may vary within the limits given in equation (8), a grain with a given set of topological parameters (n, n_d, n_s, n_q) and $n_q \neq 0$ may possess zero integrated curvature over a range of ϕ_α and ϕ_β. In addition, for a given ϕ_α and ϕ_β, a grain of topology (n, n_d, n_s, n_q) may possess zero integrated curvature in an infinity of geometries.

Just as the energetic constraints for ZIC grain formation are relaxed in grains containing quadrijunctions, the topological and geometric constraints are eased as well. For example, the Euler–Poincare rule for systems containing trijunctions and quadrijunctions requires only that $4 \leqslant \langle n \rangle \leqslant 6$. [In fact, $\langle n \rangle = (6 + 2f_q)/(1 + f_q)$ where f_q is the fraction of junctions which are quadrijunctions.] While ZIC grains with $n \leqslant 6$ must be present in an all-ZIC system, all the quadrijunction systems studied here possess multiple ZIC grain configurations with $n \leqslant 6$.

The quadrijunction stability conditions of equation (8) permit quadrijunctions to be stable over a range of angles if $\phi_\alpha + \phi_\beta$ is less than π. When junction angles can vary over a finite range of values, an infinite, disordered array of straight-sided (ZIC) polygons which obeys all topological constraints can exist. (For a 3-D example, note Polk's model for the continuous random network structure of amorphous silica [24].) Therefore, the geometric flexibility of quadrijunction-containing systems allows ZIC grains to tile space in an infinite number of different, disordered, finite arrays.

Finally, the geometric flexibility of quadrijunctions provides the resistance to topological perturbations that trijunction-only grains lack. Quadrijunctions may adjust to changes in neighbor grain shape by changing angle rather than by moving. In addition, in systems with sufficiently "flexible" quadrijunctions, ZIC grains may even be stable with respect to topological perturbations. For instance, in the system $\phi_\alpha = \phi_\beta = \pi/4$, both the (4, 4, 0, 4) and the (3, 3, 0, 3) grains are ZIC grains, so if the (4, 4, 0, 4) grain loses one of its neighbors (and hence one quadrijunction), it forms a (3, 3, 0, 3) grain and remains stable; examples of the geometric and topological stability of the (4, 4, 0, 4) ZIC grain in the $\phi_\alpha = \phi_\beta = \pi/4$ system are shown in Fig. 14. Therefore, in a quadrijunction system, it is reasonable to expect ZIC grains to form, cluster, and persist.

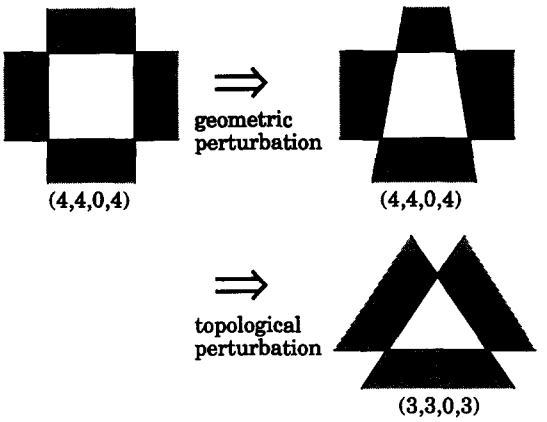

Fig. 14. The geometric and topological stability of the four-sided (white) α grain with four (gray) β neighbors, no neighbor phase switches, and four quadrijunction corners (i.e. the (4, 4, 0, 4) grain) in the $\phi_\alpha = \phi_\beta = \pi/4$ system. Due to quadrijunction flexibility, this grain can maintain zero integrated curvature despite a shape change or even the loss of a neighbor.

While the above arguments do not constitute a proof of the necessity for all-ZIC grain structures to form in systems containing quadrijunctions, they do provide a delineation of the fundamental difference between grain evolution in trijunction-only and quadrijunction systems. In addition, these arguments comprise a justification for the quadrijunction-pinning observed during simulations of systems containing quadrijunctions.

Indeed, in all the simulated systems which contain quadrijunctions grain growth was found to stop eventually. As observed in videos of microstructural evolution in quadrijunction systems, the pinning

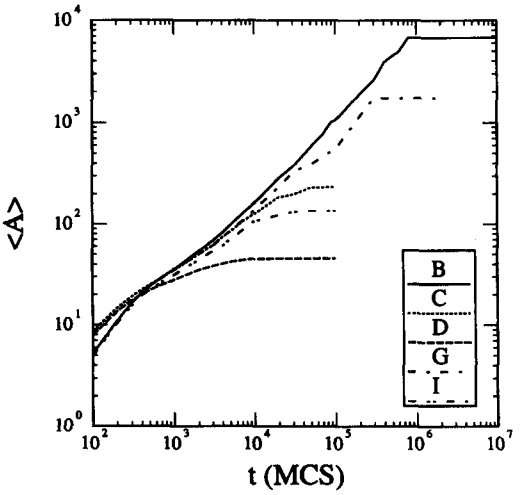

Fig. 15. The evolution of mean grain area $\langle A \rangle$ in systems containing quadrijunctions. Kinetics are depressed relative to normal, single phase growth kinetics, and grain growth eventually ceases altogether due to a loss of curvature driving force for growth.

mechanism appears to be the formation and augmentation of ZIC grain clusters. Examples of the kinetics of grain growth in quadrijunction systems are shown in Fig. 15. The onset of pinning is fairly abrupt on the logarithmic scale of this plot. The grain size at which pinning occurs depends upon the "flexibility" of the quadrijunctions; for the double wetting case (D), quadrijunction angles from 0 to π are stable in both phases, and pinning occurs at a small grain size (the microstructure in Fig. 4(g) is a pinned structure). For the system in which all microstructural features are stable (B), the quadrijunction angle range is 0.2π ($74° < \Phi < 106°$), and the pinned grain size is much larger and more variable. In the off-diagonal cases, phase asymmetry complicates the analysis of the pinned grain size, but the same trend holds: more angular flexibility (hence more available ZIC grain topologies) results in a smaller pinned grain size.

That pinning occurs due to a loss in the curvature driving force for grain boundary motion is experimentally supported by measurements of the excess curvature in the grain boundaries of the simulated systems. As an estimate of boundary curvature in the present discrete simulation method, we focus on the system activity, defined by

$$\Pi = \sum_i \sum_{S_j : S_j \neq S_i} P(S_i \rightarrow S_j) \qquad (13)$$

where the first sum is over all sites i, the second is over all sites indices S_j which differ from the current index S_i, and $P(S_i \rightarrow S_j)$ is the probability of site i changing from index S_i to a new index S_j (i.e. P is unity if the change is energetically favorable and zero otherwise). That Π scales linearly with the total grain boundary curvature at late simulation times is shown in Fig. 16 for normal grain growth. The time evolution of the normalized activity (the activity per unit length of grain boundary) is given in Fig. 17 for a number of systems. Trijunction-only systems all fall on or near

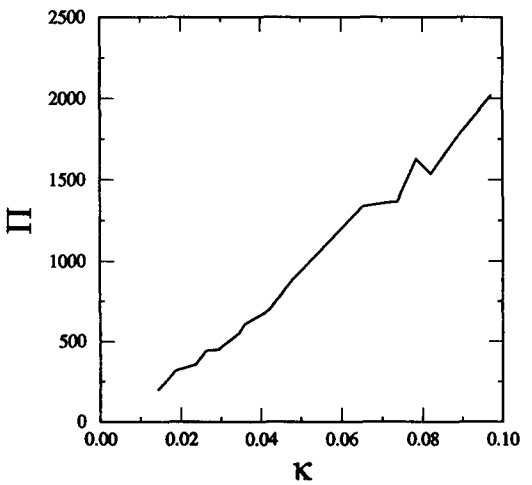

Fig. 16. The dependence of system activity Π upon grain boundary curvature κ for isotropic, single phase grain growth on a tri(1, 2) lattice. At late times (low curvatures), the system activity scales linearly with curvature.

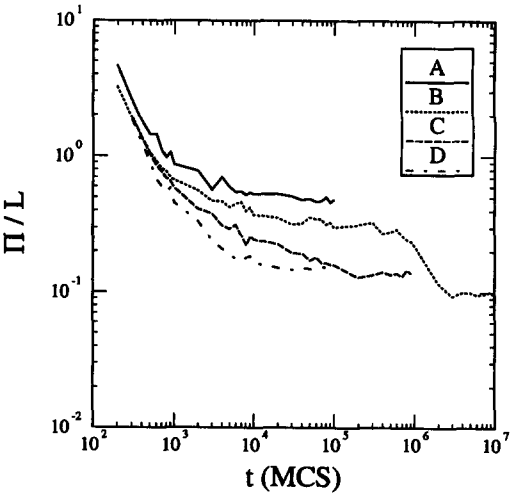

Fig. 17. The time evolution of the normalized activity (i.e. the activity Π per unit length of grain boundary L). During isotropic, single-phase grain growth, the normalized activity asymptotically approaches a constant. In systems containing quadrijunctions, the normalized activity continuously decreases until grain pinning occurs.

the upper curve in Fig. 17; the normalized activity decreases at early times and becomes constant in the scaling regime ($t \geq 10{,}000$ MCS). In systems containing quadrijunctions, the normalized activity also decreases at early times and continues to decrease until grain pinning occurs. The constant (pinned) value of the normalized activity is about the same for all pinning systems and is significantly lower than the constant value reached in trijunction-only systems. These results imply that the pinned systems not only possess far less curvature per unit length of boundary but also that the curvature characteristics of all quadrijunction-pinned systems are very similar.

To further confirm that grain pinning effects arise from a drop in driving force (curvature), we increased grain boundary fluctuations by increasing the system temperature. We found that microstructures which were pinned at a Monte Carlo temperature of zero remain pinned at elevated temperatures.

Finally, recall that normal grain growth kinetics arise from the fact that boundary velocity is proportional to curvature and curvature scales with the inverse of grain radius. Since the curvature in quadrijunction systems decreases more quickly than the inverse grain radius, we might expect to see subnormal growth kinetics in quadrijunction systems. In fact, Fig. 15 shows inhibited kinetics for all pinning systems.

7. THREE-DIMENSIONAL AND PHASE-VOLUME CONSERVED SYSTEMS

It is instructive to consider the applicability of the 2-D simulation results to 3-D systems. Since a system in any dimension tends to minimize the total length of high-energy interfaces, we would certainly expect the phase diagram of Fig. 11(a) to apply to

3-D systems. For instance, an interfacial energy controlled phase transition would occur when one grain boundary energy is the lowest interfacial energy in the system; in contrast, phases would tend to alternate when the α–β interfacial energy is lowest. Moreover, since 2-D grain junction stability criteria are the same as 3-D grain edge criteria and grain growth is spatially isotropic, we would expect the grain junction angles in a cross-section of a 3-D microstructure to be the same as those in a 2-D microstructure. However, note that there is no fundamental necessity for the topology of the 2-D system to be equivalent to that of a 3-D cross-section (although single phase 2-D grain structures do show a strong topological similarity to cross-sections of 3-D systems [13]). Finally, it is unknown whether quadrijunction pinning can occur in 3-D systems, since grain corner and edge angular conditions combine to control grain growth.

The results of this phase-volume nonconserved simulation also provide a good framework for understanding and predicting microstructural evolution in more usual phase-volume conserved systems. In particular, phase-volume is effectively conserved in the phase-volume nonconserved systems which maintain $f_\alpha \cong f_\beta \cong 0.5$ at all times [see Fig. 11(a)]. Since grain growth is an energetically driven process, we expect phase-volume conserved microstructures with $f_\alpha \cong f_\beta \cong 0.5$ to appear structurally equivalent to their phase-volume nonconserved counterparts. Even in phase-volume conserved systems in which $f_\alpha \neq f_\beta$ or in energetic regions in which phase-volume nonconserved systems undergo effective phase transitions, the evolution concepts outlined in this paper hold. For example, in a phase-volume conserved system with isolated β grain energetics ($R_\alpha = 1$, $R_\beta > 1$), we would expect to see a microstructure comprised of isolated β grains in a continuous α matrix. So while the preferred microstructural features diagram of phase-volume conserved systems may differ from Fig. 11(b), microstructures in these systems must still be consistent with the microstructures of the phase-volume nonconserved systems.

Since microstructural evolution of phase-volume conserved polycrystals may be controlled by long-range diffusion processes, the kinetics of microstructural evolution may differ greatly from phase-volume nonconserved systems. In fact, evolution kinetics will depend on the rate-limiting evolution process(es). However, since quadrijunction pinning results from a loss in the curvature driving force for boundary motion and is independent of the growth mechanism, quadrijunction pinning should occur in phase-volume conserved systems containing quadrijunctions just as in phase-volume nonconserved systems.

8. CONCLUSIONS

1. For a 2-D polycrystalline system composed of α-phase and β-phase grains, the thermodynamic stability criteria for microstructural features such as the $\alpha\alpha\alpha$, $\beta\beta\beta$, $\alpha\alpha\beta$ and $\alpha\beta\beta$ three-grain junctions and the $\alpha\beta\alpha\beta$ four-grain junction may be derived in terms of the α–α, β–β and α–β interfacial energies. Rules for the curvature-driven growth of individual grains in such systems may be derived in a similar manner to von Neumann's rule for single-phase systems.

2. Monte Carlo Potts model computer simulations provide a general method for modeling microstructural evolution in 2-D, two-phase polycrystals provided that the underlying simulation lattice is chosen with care. For the systems studied here, the triangular lattice with equal first and second neighbor interactions was found to be an appropriate simulation lattice. Simulated microstructures are realistic and consistent with thermodynamic predictions; that is, they contain only thermodynamically stable features, trijunction angles are near their equilibrium values, and quadrijunction angles fall within their stable ranges.

3. For systems in which the α–α and β–β interfacial energies are equal or in which the α–β interfacial energy is the lowest energy, microstructures contain all thermodynamically stable features and the volume fractions of each phase are approximately equal. Phase arrangements in such systems may vary from phase clustering to a random phase distribution to alternating phases.

4. When one grain boundary energy is the lowest interfacial energy, the polycrystal undergoes an interfacial energy induced phase transition to the phase of low boundary energy. When one boundary energy and the α–β interfacial energy are equal and low, the system isolates the high boundary energy phase grains in a matrix of the low boundary energy phase. Once isolated. these second phase grains grow or shrink normally. Systems such as these in which the volume fractions of α and β are not nearly equal may not contain all the microstructural features thermodynamically accessible to them.

5. Since the bulk free energies of α and β are equivalent, the interfacial energies control both the phases and the microstructural features present in a phase-volume nonconserved system. Thus, a phase diagram for the α–β system may be plotted in terms of the interfacial energy ratios; four distinct phase fields occur. Likewise, the microstructural features present in an evolved structure are completely described by the interfacial energy ratios.

6. The kinetics of microstructural evolution in the two-phase, phase-volume nonconserved system are much more complex than in normal grain growth. Despite great differences in junction geometries, polycrystalline systems which contain only trijunctions evolve with essentially normal, single-phase grain growth kinetics; the topology of such systems is found to be similar to the topology of normal, single phase grain systems. In contrast, structures which contain quadrijunctions eventually stop evolving due to the angular flexibility of quadrijunctions. We

conclude that grain growth cannot cease when grain junctions angles are thermodynamically fixed; grain growth can and does cease when grain junction angles may flex.

7. Predictions concerning 3-D and phase-volume conserved systems may be made on the basis of the 2-D phase-volume nonconserved results.

Acknowledgements—EAH's work has been supported in part by a National Science Foundation Graduate Research Fellowship and by an IBM Predoctoral Fellowship in Scientific Computing. Many thanks to Dr A. D. Rollett for discussions of kinetics and kinematics.

REFERENCES

1. C. S. Smith, in *Metal Interfaces*, p. 65. Am. Soc. Metals, Cleveland, Ohio (1952).
2. J. von Neumann, in *Metal Interfaces*, p. 108. Am. Soc. Metals, Cleveland, Ohio (1952).
3. W. W. Mullins, *Scripta metall.* **22,** 1441 (1988).
4. J. W. Cahn, *Acta metall. mater.* **39,** 2189 (1991).
5. J. E. Taylor, *Acta metall. mater.* **40,** 1475 (1992).
6. J. W. Cahn, E. A. Holm and D. J. Srolovitz, in *Proc. Int. Conf. on Grain Growth in Polycrystalline Materials*, p. 141. Trans Tech, Brookfield, Vt (1992).
7. J. W. Gibbs, *Collected Works*, Vol. 1, pp. 287–289. Yale Univ. Press, New Haven, Conn. (1948).
8. C. S. Smith, *Trans. Am. Inst. Min. Engrs* **175,** 15 (1948).
9. P. J. Clemm and J. C. Fisher, *Acta metall.* **3,** 70 (1955).
10. J. E. Taylor, in *Global Analysis and its Applications*, Vol. II, p. 271. IEAE, Vienna (1974).
11. M. P. Anderson, D. J. Srolovitz, G. S. Grest and P. S. Sahni, *Acta metall.* **32,** 783 (1984).
12. D. J. Srolovitz, M. P. Anderson, P. S. Sahni and G. S. Grest, *Acta metall.* **32,** 793 (1984).
13. M. P. Anderson, G. S. Grest and D. J. Srolovitz, *Phil. Mag. B* **59,** 293 (1989).
14. A. D. Rollett, D. J. Srolovitz and M. P. Anderson, *Acta metall.* **37,** 1227 (1989).
15. P. S. Sahni, D. J. Srolovitz, G. S. Grest, M. P. Anderson and S. A. Safran, *Phys. Rev. B* **28,** 2705 (1983).
16. E. A. Holm, J. A. Glazier, D. J. Srolovitz and G. S. Grest, *Phys. Rev. A* **43,** 2662 (1991).
17. G. S. Grest, M. P. Anderson and D. J. Srolovitz, *Phys. Rev. B.* **38,** 4752 (1988).
18. G. N. Hassold and E. A. Holm, *Comput. Phys.*, in press.
19. S. Ling and M. P. Anderson, personal communication.
20. W. W. Mullins and J. Viñals, *Acta metall.* **37,** 991 (1989).
21. M. Hillert, *Acta metall.* **13,** 227 (1965).
22. J. W. Cahn and G. E. Padawer, *Acta metall.* **13,** 1091 (1965).
23. D. Harker and E. Parker, *Trans. Am. Soc. Metals* **34,** 156 (1945).
24. D. E. Polk, *J. Non-Cryst. Solids* **5,** 365 (1971).